H_2S Splitting Hot Paper

DOI: 10.1002/anie.201400571

An Integrated Photoelectrochemical–Chemical Loop for Solar-Driven Overall Splitting of Hydrogen Sulfide**

Xu Zong, Jingfeng Han, Brian Seger, Hongjun Chen, Gaoqing (Max) Lu, Can Li, and Lianzhou Wang**

Abstract: *Abundant and toxic hydrogen sulfide (H_2S) from industry and nature has been traditionally considered a liability. However, it represents a potential resource if valuable H_2 and elemental sulfur can be simultaneously extracted through a H_2S splitting reaction. Herein a photochemical-chemical loop linked by redox couples such as Fe^{2+}/Fe^{3+} and I^-/I_3^- for photoelectrochemical H_2 production and H_2S chemical absorption redox reactions are reported. Using functionalized Si as photoelectrodes, H_2S was successfully split into elemental sulfur and H_2 with high stability and selectivity under simulated solar light. This new conceptual design will not only provide a possible route for using solar energy to convert H_2S into valuable resources, but also sheds light on some challenging photochemical reactions such as CH_4 activation and CO_2 reduction.*

Hydrogen sulfide (H_2S) is an abundant chemical produced by industry and occurring in nature. Although H_2S represents potential resources of two elements which individually have significant economic value, its potential has been hardly realized by community because of its extremely toxic and irritating nature and existing treating techniques. However, there is an increasing recognition that H_2S could become a potentially valuable chemical if a process that can simultaneously extract H_2 and elemental sulfur (S) from H_2S was developed.[1] At present, H_2S is primarily treated with Claus process wherein it is partially oxidized to yield elemental S and water.[2] Although S can be extracted from H_2S with this approach, one of the disadvantages is the loss of H_2 in H_2S during the conversion. Therefore, it is highly desirable to develop a sustainable and cost-effective process to simultaneously recover H_2 and S from H_2S.

The H_2S splitting reaction ($\Delta G^0 = 33\ kJ\,mol^{-1}$) is thermodynamically less stringent compared with the H_2O splitting reaction ($\Delta G^0 = 273\ kJ\,mol^{-1}$).[3] To date, different approaches including thermal,[4] thermochemical,[5] electrochemical,[6] photochemical,[7] and plasmochemical[8] decomposition methods have been investigated for H_2S splitting. Among these approaches, photochemical splitting of H_2S is attractive because of its potential of using abundant solar energy.[9] The prevalent reaction scheme for photochemical H_2S splitting is shown in Scheme 1a. In the first step, H_2S is chemically absorbed in alkali solution (such as NaOH solution) to generate S^{2-}. In the second step, S^{2-} is oxidized by photogenerated holes to polysulfide and protons are reduced to H_2. Although H_2 can be extracted from H_2S using this approach, it is difficult to recover S because of the highly basic nature of the absorption solution.[10] Moreover, the generation of polysulfide by-products and the shielding of light by the polysulfide ions inevitably introduce new environmental and technical challenges, which makes this method less appealing. So far, the development of a sustainable and economically viable photochemical approach that can split H_2S to produce H_2 and S simultaneously still remains a challenging task.

Herein we report an innovative approach that can simultaneously extract H_2 and S from toxic H_2S by using solar energy. Through the integration of photoelectrochemical and chemical reactions linked by I^-/I_3^- or Fe^{2+}/Fe^{3+} redox couples, H_2S can be successfully split into S and H_2 with high stability and selectivity. To our knowledge, this is the first reported photoelectrochemical process for overall splitting of H_2S without the necessity of post-treating sulfur-based aqueous solution. This conceptually provides an alternative

[*] Dr. X. Zong, Dr. H. J. Chen, Prof. G. Q. (Max) Lu, Prof. L. Z. Wang
Nanomaterials Centre, School of Chemical Engineering and Australian Institute for Bioengineering and Nanotechnology
The University of Queensland
QLD 4072 (Australia)
E-mail: l.wang@uq.edu.au
J. F. Han, Prof. Dr. C. Li
State Key Laboratory of Catalysis
Dalian Institute of Chemical Physics
Chinese Academy of Sciences and Dalian Laboratory for Clean Energy
Dalian 116023 (China)
E-mail: canli@dicp.ac.cn
Homepage: http://www.canli.dicp.ac.cn
J. F. Han
Graduate University of Chinese Academy of Sciences
Beijing 100049 (China)
Dr. B. Seger
Department of Physics, CINF, Technical University of Denmark
2800 Kongens Lyngby (Denmark)

[**] This project was supported by the Australian Research Council (through its DP and FT programs) and Queensland State Government Smart State program (NIRAP). This work was performed in part at the Qld node of the Australian National Fabrication Facility. We gratefully acknowledge the Danish Ministry of Science for funding the Catalysis for Sustainable Energy (CASE) initiative and the Danish National Research Foundation for founding The Center for Individual Nanoparticle Functionality. We also thank Thomas Pedersen (DTU) for providing p-n junction Si wafers.

Supporting information for this article is available on the WWW under http://dx.doi.org/10.1002/anie.201400571.

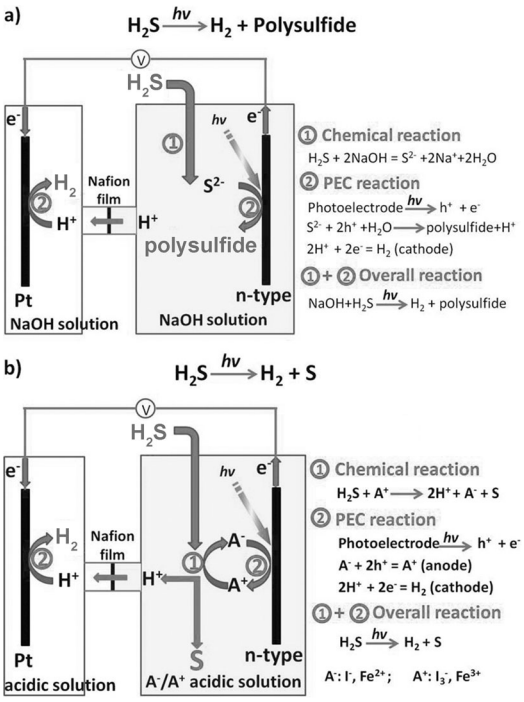

Scheme 1. a) Conventional photoelectrochemical approach, and b) proposed photoelectrochemical–chemical loop for H_2S splitting on a n-type photoelectrode linked with redox couples.

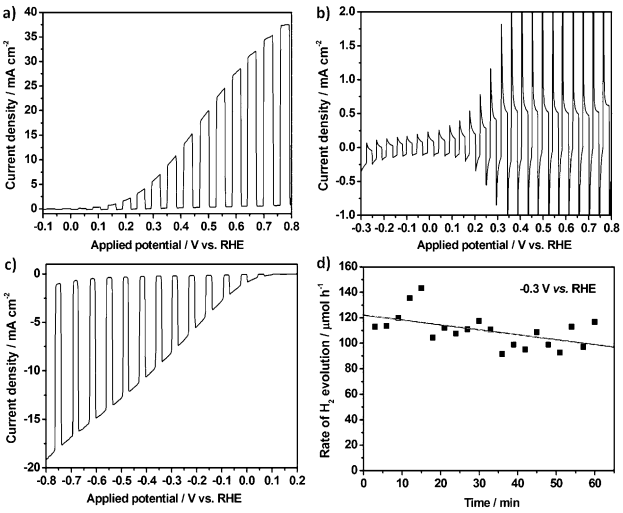

Figure 1. a–c) Current–potential curves of a) n-Si electrode with PEDOT coating in 0.2 M $FeSO_4$ acidic solution, b) n-Si electrode with PEDOT coating in 0.5 M H_2SO_4 solution, c) p-Si electrode with Pt catalyst with 0.2 M $FeSO_4$ acidic solution in the counter compartment, and d) the rate of H_2 evolution measured based on GC analysis. Light source: AM1.5G, 100 mW cm^{-2}.

approach for converting abundant and toxic H_2S to valuable chemicals using solar energy.

Our process of converting H_2S to H_2 and S consists of two integrated reactions as schematically shown in Scheme 1b and Scheme S1 in the Supporting Information. The first reaction is a simple chemical reaction (reaction 1) that can efficiently trap and selectively convert H_2S to S and protons by the oxidation state of redox couples(I^-/I_3^- or Fe^{2+}/Fe^{3+}). The second reaction is a photoelectrochemical reaction (reaction 2) that can reduce protons to generate H_2. In the meantime, the reduction state of the redox couples is restored to the initial oxidation state by the photogenerated holes. Thus with the link of the redox couples, the net reaction is the overall splitting of H_2S to produce both H_2 and S using solar energy.

As a proof of concept study, we first investigated the photoelectrochemical and chemical reactions, respectively (experimental details are given in the Supporting Information). Functionalized p-type Si (p-Si) and n-type Si (n-Si) were used for the photoelectrochemical measurements (Figure S1). (3,4-ethylenedioxythiophene) (PEDOT) was coated on n-Si because of its functionality of stabilizing inorganic photoanodes against photochemical corrosion in corrosive electrolytes.[11] As shown in Figure 1a, n-Si coated with PEDOT delivered a photocurrent of about 35 mA cm^{-2} at an applied potential of 0.8 V vs. the reversible hydrogen electrode (RHE) in an acidic $FeSO_4$ electrolyte. A photocurrent of a similar level was also obtained when using an acidic KI electrolyte (Figure S2). However, when H_2SO_4 solution was used, only a negligible photocurrent of about 0.5 mA cm^{-2} was obtained at the same applied potential (Figure 1b). These results are easy to understand considering that the oxidation of Fe^{2+} to Fe^{3+} (or I^- to I_3^-) is kinetically favorable. Therefore, it is reasonable to conclude that most of the anodic photocurrent is ascribed to the photooxidation of Fe^{2+} to Fe^{3+} (or I^- to I_3^-). Photoelectrochemical measurements were also conducted on p-Si photocathode with electrodeposited Pt catalyst. As shown in Figure 1c, the p-Si cathode delivered a photocurrent of about 17.0 mA cm^{-2} at an applied potential of −0.8 V vs. RHE in the H_2SO_4 electrolyte. At the same time, vigorous bubbles of H_2 were observed on the surface of the p-Si electrode and the KI electrolyte in the anodic compartment rapidly turned red with prolonged testing, indicating the generation of I_3^-.

To confirm the nature and amount of the evolved gases, we purged the gases in the two compartments, respectively, into gas chromatography (GC) for analysis. Because of the better stability of the p-Si photocathode compared with that of the PEDOT/n-Si photoanode in this study (Figure S2b, S4, S5a), we used a p-Si photocathode for this long-term investigation. H_2 was identified to be the only gaseous product in the cathodic compartment. The rate of H_2 evolution decreased gradually with prolonged irradiation and was estimated to be about 90–120 μmol h^{-1} (Figure 1d). Because of the relatively large dead volume of the reactors, only part of the H_2 gas in the reactor can be sampled into GC for analysis. Therefore, the rate of H_2 evolution calculated from the GC analysis was a little lower than that calculated based on the photocurrent. However, this result does provide clear evidence for the hydrogen produced. We also analyzed the gas in the anodic compartment while no signals (such as O_2 or N_2) were observed (Figure S3b), testifying that Fe^{3+} (or I^-) instead of O_2 was produced. This result was further confirmed by enhanced UV/Vis absorption ascribed to the increased generation of Fe^{3+} (Figure S5b). Because of the presence of the Nafion membrane sandwiched between the

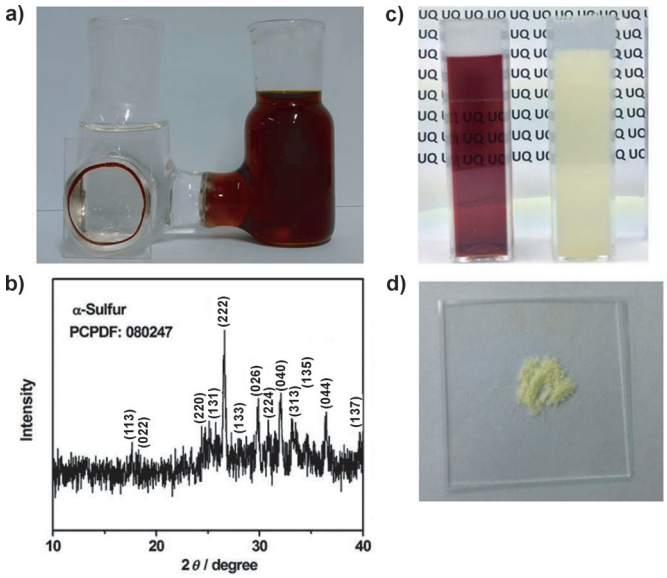

Figure 2. a) Picture showing the generations of I_3^- after chronoamperometric test on p-Si photocathode. Photocathode is located in the left compartment and the counter electrode in the right compartment. b) Picture showing the generation of yellowish turbid in the right cuvette after bubbling H_2S gas into aqueous solution containing I_3^- in the left cuvette. C) XRD pattern of the yellowish S powder. D) The picture of the resultant yellowish S powder.

two compartments, the production of Fe^{3+} (or I_3^-) is anticipated to be confined in the compartment where photooxidation reaction takes place (Figure 2a). This design will prohibit the backward reaction of Fe^{3+} to Fe^{2+} (or I_3^- to I^-) on the photocathode and ensure that most of the Fe^{3+} or I_3^- could be used for the subsequent chemical reactions.

After confirming that H_2 can be produced with the simultaneous generation of Fe^{3+} or I_3^-, we then proceeded with the second step of our design by slowly bubbling H_2S into the electrolytes containing Fe^{3+} or I_3^-. Figure 2b shows that after bubbling H_2S into the electrolytes containing I_3^-, the bright red solution turned yellow turbid. The X-ray diffraction (XRD) peaks of the yellowish (Figure 2c) can be indexed to α-S and match well with those of commercial S (Figure S6), indicating the successful production of S by chemically treating H_2S with the solution obtained in the photochemical reactions. Similarly, α-S can also be obtained when trapping H_2S with electrolyte that contains Fe^{3+}. Therefore, the chemical energy stored in the form of Fe^{3+} or I_3^- can be liberated to oxidize H_2S chemically to produce S and protons according to Scheme 1b. Consequently, Fe^{3+} or I_3^- ions were restored to their reduced state to close the loop. Thus by repeating the photoelectrochemical and chemical reactions linked by the redox couples, H_2S can be directly split into H_2 and S continuously.

To achieve sustainable H_2S splitting, it is crucial to find a robust photoelectrode that could sustain photochemical and chemical corrosions. The PEDOT/n-Si electrode degraded either in $FeSO_4$ or KI electrolytes with prolonged irradiation (Figures S2b and S4a). A similar trend was observed for the p-Si photocathode (Figure S5a). For n-Si, it is possible to further improve its performance by a structural modification technique or by optimizing the coating process.[12] For the p-Si photocathode, its performance and stability property can be greatly improved by achieving a thin surface n^+ doping, depositing protective TiO_2/Ti coating and loading H_2-evolution catalysts.[13] We then systematically investigated the performance of the Pt/TiO_2/Ti/n^+p-Si photocathode. As shown in Figure 3a, the onset potential of the Pt/TiO_2/Ti/n^+p-Si photocathode was drastically reduced to about 0.5 V vs. RHE. Moreover, a saturation photocurrent of 24 mA cm^{-2}

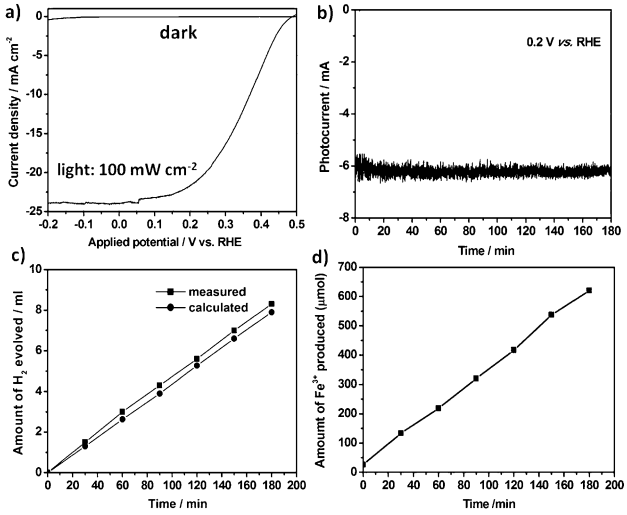

Figure 3. a) Current–potential curves, and b) chronoamperometry of the Pt/TiO_2/Ti/n^+p-Si electrode at an applied potential of 0.2 V vs. RHE in a three-electrode system. c) The amount of gas evolved from the photocathode compartment. ■ represents the values measured and ● represents the values calculated from the photocurrent. d) The rate of Fe^{3+} generation based upon the UV/Vis absorption spectra analysis. Electrolyte: 0.2 M $FeSO_4$ acidic solution. Light source: AM1.5G, 100 mW cm^{-2}.

was obtained at an applied potential of as low as 0 V vs. RHE. Chronoamperometric scans showed that the Pt/TiO_2/Ti/n^+p-Si electrode showed a quite stable cathodic photocurrent compared with the p-Si electrode (Figure 3b). Owning to the stable and excellent performance of the present electrode, we can quantitatively measure the amount of the gas products using a simple water displacement method in an air-tight reactor. Figure 3c shows the time course of H_2 evolution on Pt/TiO_2/Ti/n^+p-Si at an applied potential of 0.2 V vs. RHE. As expected, steady H_2 evolution was achieved and a total amount of 8.3 mL of H_2 gas was obtained during the three hour duration of the reaction. The volume of H_2 gas measured with the water displacement method is slightly higher than that calculated (7.9 mL) based upon the photocurrent shown in Figure 3b. The UV/Vis absorption analysis of the aqueous solution in the counter electrode compartment indicated that Fe^{3+} ions were produced with a steady rate and a total amount of 590 μmol Fe^{3+} produced in three hours. This value is about 80% of the theoretical value, which is possibly because of the resistive losses in the electrolyte and Nafion membrane. Similar results were obtained when using KI as the electrolyte for the durability test (Figure S4). Elemental sulfur may play

a role in contributing to the photocurrent observed.[14] However, as the photoactivity of the sulfur electrode is normally much smaller than that of the Si electrode, the influence should be negligible.

In the above study, we investigated the photochemical and chemical reactions respectively to verify our conceptual design. However, it still remains a question whether the two reactions can be integrated to achieve a loop. We then carried out photoelectrochemical measurements on the $Pt/TiO_2/Ti/n^+p$-Si electrode with simultaneous bubbling H_2S gas into the anodic compartment. As shown in Figure 4a, the $Pt/TiO_2/Ti/n^+p$-Si electrode showed a very stable cathodic photocurrent for generating H_2. Meanwhile, the clear solution in the anodic compartment rapidly turned to a turbid yellowish upon simultaneous injection of H_2S gas (compartment (1) in Figure 4b). However, the anodic compartment still retained the characteristic color of I_3^- without bubbling H_2S gas (compartment (3) in Figure 4c). Therefore, the photogenerated I_3^- can rapidly react with H_2S to produce S in an in situ manner in the counter electrode compartment. Because of the separation of the Nafion membrane, H_2 and S can be produced in the two compartments, respectively, while protons can transfer through the Nafion membrane to achieve equilibrium for the proton reduction reaction in the cathodic compartment. We also conducted control experiments by directly splitting H_2S on the photoelectrode in acidic solution without the use of the redox couples. However, this approach was unsuccessful because of the very low solubility of H_2S in acidic solution. On this basis, the present design apparently has the advantages over other photochemical methods for H_2S splitting in terms of the effectiveness and the appreciable nature of the end products. However, to make it viable commercially, we should not underestimate the technological challenges such as the separation and purification of S from the aqueous solution.

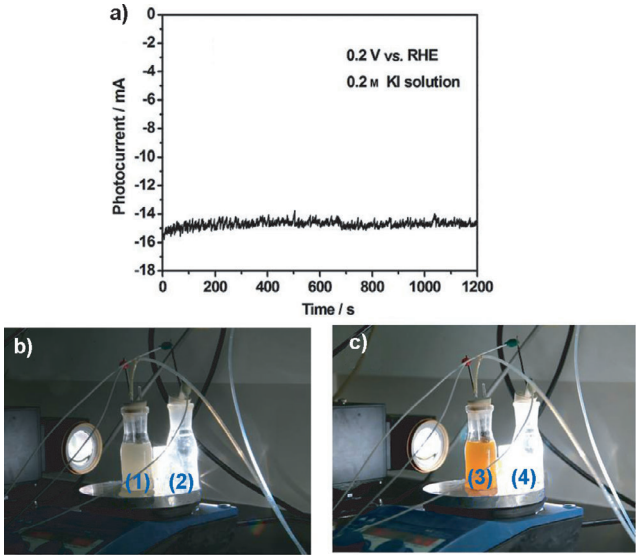

Figure 4. a) Chronoamperometry at an applied potential of 0.2 V vs. RHE in a three-electrode system using the $Pt/TiO_2/Ti/n^+p$-Si electrode. H_2S was bubbled into the solution in the counter electrode compartment simultaneously. b) Picture showing the simultaneous generation of S and H_2 with H_2S bubbling into the counter electrode compartment. (1) and (2) indicate the anodic and cathodic compartments, respectively. c) Picture showing the accumulation of I_3^- without H_2S bubbling. (3) and (4) indicate the anodic and cathodic compartments, respectively. Electrolyte: 0.2 M KI acidic solution. The irradiation area is approximately 0.283 cm^2. The intensity of the light is estimated to be about 2.5 sun.

In summary, we demonstrated an effective route of using solar energy to convert abundant and toxic H_2S to valuable chemical resources in a proof of concept study. With the link of redox couples such as Fe^{2+}/Fe^{3+} and I^-/I_3^-, the reaction loop for H_2S splitting was realized by coupling photoelectrochemical H_2 production and H_2S absorption chemical redox reactions. This design of converting hazardous "waste" into valuable chemicals also provides useful insights into some challenging reactions such as photochemical CO_2 reduction and CH_4 activation.

Received: January 19, 2014
Revised: February 25, 2014
Published online: March 26, 2014

Keywords: hydrogen generation · H_2S splitting · photoelectrochemistry · solar energy · sulfur

[1] a) G. J. Ma, H. J. Yan, J. Y. Shi, X. Zong, Z. B. Lei, C. Li, *J. Catal.* **2008**, *260*, 134–140; b) J. Zaman, A. Chakma, *Fuel Process. Technol.* **1995**, *41*, 159–198.
[2] A. Pieplu, O. Saur, J. C. Lavalley, O. Legendre, C. Nedez, *Catal. Rev. Sci. Eng.* **1998**, *40*, 409–450.
[3] H. Shiina, M. Oya, K. Yamashita, A. Miyoshi, H. Matsui, *J. Phys. Chem.* **1996**, *100*, 2136–2140.
[4] E. A. Fletcher, J. E. Noring, J. P. Murray, *Int. J. Hydrogen Energy* **1984**, *9*, 587–593.
[5] a) H. Wang, *Int. J. Hydrogen Energy* **2007**, *32*, 3907–3914; b) T. Chivers, J. B. Hyne, C. Lau, *Int. J. Hydrogen Energy* **1980**, *5*, 499–506; c) L. M. Alshamma, S. A. Naman, *Int. J. Hydrogen Energy* **1990**, *15*, 1–5.
[6] a) K. Petrov, S. Srinivasan, *Int. J. Hydrogen Energy* **1996**, *21*, 163–169; b) D. W. Kalina, E. T. Maas, *Int. J. Hydrogen Energy* **1985**, *10*, 157–162; c) H. Y. Huang, Y. Yu, K. H. Chung, *Energy Fuels* **2009**, *23*, 4420–4425.
[7] a) I. Tsuji, H. Kato, H. Kobayashi, A. Kudo, *J. Am. Chem. Soc.* **2004**, *126*, 13406–13413; b) H. J. Yan, J. H. Yang, G. J. Ma, G. P. Wu, X. Zong, Z. B. Lei, J. Y. Shi, C. Li, *J. Catal.* **2009**, *266*, 165–168; c) J. F. Reber, M. Rusek, *J. Phys. Chem.* **1986**, *90*, 824–834; d) J. F. Reber, K. Meier, *J. Phys. Chem.* **1984**, *88*, 5903–5913; e) Z. Lei, W. You, M. Liu, G. Zhou, T. Takata, M. Hara, K. Domen, C. Li, *Chem. Commun.* **2003**, 2142–2143; f) S. V. Tambwekar, M. Subrahmanyam, *Int. J. Hydrogen Energy* **1997**, *22*, 959–965.
[8] a) G. B. Zhao, S. John, J. J. Zhang, J. C. Hamann, S. S. Muknahallipatna, S. Legowski, J. F. Ackerman, M. D. Argyle, *Chem. Eng. Sci.* **2007**, *62*, 2216–2227; b) E. L. Reddy, V. M. Biju, C. Subrahmanyam, *Appl. Energy* **2012**, *95*, 87–92; c) T. Nunnally, K. Gutsol, A. Rabinovich, A. Fridman, A. Starikovsky, A. Gutsol, R. W. Potter, *Int. J. Hydrogen Energy* **2009**, *34*, 7618–7625.
[9] a) X. B. Chen, S. H. Shen, L. J. Guo, S. S. Mao, *Chem. Rev.* **2010**, *110*, 6503–6570; b) X. Zong, H. J. Yan, G. P. Wu, G. J. Ma, F. Y. Wen, L. Wang, C. Li, *J. Am. Chem. Soc.* **2008**, *130*, 7176–7177; c) A. Kudo, Y. Miseki, *Chem. Soc. Rev.* **2009**, *38*, 253–278.

[10] a) P. Dubois, J. P. Lelieur, G. Lepoutre, *Inorg. Chem.* **1987**, *26*, 1897 – 1902; b) P. Dubois, J. P. Lelieur, G. Lepoutre, *Inorg. Chem.* **1988**, *27*, 1883 – 1890.
[11] S. Mubeen, J. Lee, N. Singh, M. Moskovits, E. W. McFarland, *Energy Environ. Sci.* **2013**, *6*, 1633 – 1639.
[12] a) T. Yang, H. Wang, X. M. Ou, C. S. Lee, X. H. Zhang, *Adv. Mater.* **2012**, *24*, 6199 – 6203; b) K. Q. Peng, S. T. Lee, *Adv. Mater.* **2011**, *23*, 198 – 215; c) X. J. Li, W. H. Lu, W. L. Dong, Q. Chen, D. Wu, W. Z. Zhou, L. W. Chen, *Nanoscale* **2013**, *5*, 5257 – 5261.
[13] a) B. Seger, A. B. Laursen, P. C. K. Vesborg, T. Pedersen, O. Hansen, S. Dahl, I. Chorkendorff, *Angew. Chem.* **2012**, *124*, 9262 – 9265; *Angew. Chem. Int. Ed.* **2012**, *51*, 9128 – 9131; b) B. Seger, T. Pedersen, A. B. Laursen, P. C. K. Vesborg, O. Hansen, I. Chorkendorff, *J. Am. Chem. Soc.* **2013**, *135*, 1057 – 1064.
[14] G. Liu, P. Niu, Li. C. Yin, H. M. Cheng, *J. Am. Chem. Soc.* **2012**, *134*, 9070 – 9073.

